

Spectral-spatial diffusion in inhomogeneously broadened systems*

T. Holstein, S. K. Lyo, and R. Orbach

Department of Physics, University of California, Los Angeles, California 90024

(Received 21 June 1976)

Most phonon-assisted spectral transfer rates across an inhomogeneously broadened line are proportional to the inverse square of the energy change. The time-dependent optical emission profile is calculated exactly for a rectangular line shape for these processes. Numerical solutions are required for other line shapes (e.g., a Gaussian as found in ruby). They are exhibited as a function of time for a variety of initial excitation energies at different positions across the optical line.

I. INTRODUCTION

In a previous publication¹ (to be referred to as I), a number of phonon-assisted spatial energy-transfer processes were computed for inhomogeneously broadened spectral lines in solids. For the case of ruby, a two-phonon process was predicted to dominate, leading to a transfer rate inversely proportional to the square of the energy change in the excitation transfer process. The peculiar character of this energy dependence has led us to examine the evolution in time of the emission line profile for the case of sharp-line (e.g., laser) excitation. We shall assume that the variations in environment which lead to the inhomogeneous broadening are microscopically random, so that there is no correlation between transition energy and spatial position. This allows us to average over all spatial positions and to focus solely on the energy-mismatch dependence of the transfer rate.

A general expression for the time development of the emission line shape was first written down by Motegi and Shionoya.² Unfortunately one cannot solve their equation for an arbitrary equilibrium line shape. We have been able to obtain an exact solution, however, for the time evolution of the emission line profile for a rectangular density of states with arbitrary initial excitation. We have also set up a numerical iteration procedure for the time development of the excitation function for an arbitrary density of states.

The general features of our solutions are interesting. For a rectangular shape, the inverse-square energy dependence of the transfer rate leads to a continuously spreading excitation across the line. The rate of spread turns out to be independent of the "jump" energy, being nearly the same for a single jump as for a large number of small jumps covering the same energy interval. This curious result is peculiar to the inverse-square energy dependence of the transfer rate (actually a rather general feature of two-phonon-

assisted energy transfer¹), and to the rectangular density-of-states model. Should the transfer rate fall off more rapidly with energy change, the result approaches the more conventional small-energy-change diffusion limit.

For the case of an inhomogeneous line of Gaussian shape (as found in ruby, for example), the slowly varying inverse-square dependence of the transfer rate is overwhelmed by the much more rapidly varying Gaussian density of final states. The initial sharp excitation line is observed (on the computer) to decay monotonically, while the spectrally (spatially) transferred energy appears first near the center of the equilibrium emission line profile, but is shifted slightly towards the initial excitation line position. The emission line profile then develops into the equilibrium Gaussian line shape. In general, the farther the initial excitation is from the emission line center, the longer the transfer process takes to complete its time evolution.

The two-phonon-assisted spectral (spatial) transfer process considered above is interestingly the inverse of the problem of radiation trapping in planetary nebulas.^{3,4} In this physical situation, two conditions obtain: (a) collision broadening is quite negligible, and (b) the spatial dimensions are sufficiently large that at the absorption edge of a Doppler-broadened line (the frequency at which the opacity of the enclosure is ~ 1), the line shape is dominated by natural broadening. In such a limit, excitations diffuse slowly across the line profile in small steps, appropriate to Doppler shifts arising from absorption-reemission processes. In the present problem, by way of contrast, diffusion to the wings for phonon-assisted transfer takes place in essentially a single step.

We formulate the expression for the time evolution of the emission line profile in Sec. II. The exact solution for a rectangular density of states is derived in Sec. III, along with a discussion of its significance. A numerical iterative solution of the time-evolution expression is formulated in

Sec. IV. Various initial conditions are analyzed and representative time developments are exhibited. Section V summarizes our results and reviews our conclusions.

II. TIME DEVELOPMENT OF THE EMISSION SPECTRUM

We wish to calculate the emission spectrum of an excited level subject to an initial excitation of arbitrary spectral shape. We denote the equilibrium emission line shape for the inhomogeneously broadened line by $g(E)$, and the energy transfer rate from a packet with central energy E' to a packet with energy E by $W(E - E')$. We denote the emission probability function by $P(E, t)$. Our definition differs from that of Ref. 2 because we absorb the line-shape factor $g(E)$ into the emission probability function, whereas Motegi and Shionoya separate $P(E, t)$ into the excitation probability of a given packet, $p(E, t)$, times the probability of finding that packet, equal to the line-shape function $g(E)$. Thus, $[P(E, t)]^{\text{ours}} = [p(E, t)]^{\text{theirs}} g(E)$. Given this distinction, the time dependence of $P(E, t)$ is given by²

$$\frac{dP(E, t)}{dt} = \int [g(E)W(E - E')P(E', t) - g(E')W(E' - E)P(E, t)] dE'. \quad (1)$$

We are interested in linewidths much smaller than $k_B T$, so that $W(E - E') = W(E' - E)$. According to I, the energy-transfer rate varies inversely as the square of the energy mismatch. We write, therefore,

$$W(E - E') = W_0 \frac{\gamma/\pi}{(E - E')^2 + \gamma^2}. \quad (2)$$

We have inserted a "width" γ for normalization and convergence purposes. It will turn out that this convergence parameter will play no essential role in our solutions. Comparing with I, for example,

$$W_0 \gamma = \pi J^2 W_{\bar{E}-2\bar{A}} \quad (3)$$

for ruby, where J is a mean site-site exchange coupling (varying rapidly with concentration), and $W_{\bar{E}-2\bar{A}}$ is the phonon-induced excitation rate within the 2E manifold, varying as $e^{-\delta/k_B T}$, where $\delta = E(2\bar{A}) - E(\bar{E})$. This form for $W_0 \gamma$ corresponds to only one of a number of two-phonon-assisted energy-transfer processes. The "nonresonant" (see I for a pictorial sketch) and Raman processes generate a T^7 temperature dependence for $W_0 \gamma$. The latter is proportional to the square of the difference in phonon couplings between the ground and excited levels. Our numerical estimates indicate that (3) dominates for ruby, for example, at rea-

sonably low temperatures ($T \lesssim 10$ K).

In the following sections, we integrate (1), using a Lorentzian form for the initial emission probability function $P(E, 0)$:

$$P(E, 0) = \frac{\gamma_0/\pi}{(E - E_0)^2 + \gamma_0^2}. \quad (4)$$

Our results will not depend sensitively upon the initial conditions. We have used Gaussian shapes as well, with little significant change in the emission time-development profile (except for an increase in the time scale). We shall choose $\gamma = \gamma_0$ for convenience, and the width of $g(E)$ will be taken considerably larger than γ , so that the initial excitation width is small compared to the equilibrium emission width.

III. RECTANGULAR DENSITY OF STATES. EXACT SOLUTION FOR THE TIME DEVELOPMENT OF THE EMISSION LINE PROFILE

In the limit of a simple rectangular density of states [i.e., $g(E) = 1/\Delta$ for $-\Delta/2 < E < \Delta/2$, and 0 otherwise], one can solve (1) for $|E| \ll \Delta$. In this limit, (1) becomes a simple convolution. Defining

$$P(E, t) = \frac{1}{\sqrt{2\pi}} \int_{-\infty}^{\infty} P(s, t) e^{-isE} ds, \quad (5)$$

(1) reduces to

$$\frac{dP(s, t)}{dt} = \left(\sqrt{2\pi} \frac{W(s)}{\Delta} - \frac{W_0}{\Delta} \right) P(s, t), \quad (6)$$

which can be integrated immediately. Here, $W(s)$ is the Fourier transform of (2), equaling $(1/\sqrt{2\pi}) \times W_0 e^{-\gamma|s|}$. One finds

$$P(s, t) = P(s, 0) e^{-W_0 t/\Delta} \exp\left(\frac{W_0 t}{\Delta} e^{-\gamma|s|}\right) \\ = \frac{1}{\sqrt{2\pi}} e^{-W_0 t/\Delta} \sum_{n=0}^{\infty} \frac{(W_0 t/\Delta)^n}{n!} e^{-(\gamma_0 + n\gamma)|s| + isE_0}, \quad (7)$$

where we have used $P(s, 0) = (1/\sqrt{2\pi}) e^{-\gamma_0|s| + isE_0}$.

Taking the inverse Fourier transform, we find

$$P(E, t) = e^{-W_0 t/\Delta} \sum_{n=0}^{\infty} \frac{(W_0 t/\Delta)^n}{n!} \frac{(\gamma_0 + n\gamma)/\pi}{(E - E_0)^2 + (\gamma_0 + n\gamma)^2}. \quad (8)$$

This solution has some remarkable features. The summand is peaked for $n = W_0 t/\Delta$, the more sharply the larger n . Because W_0 enters as the n th power, the n th term can be interpreted as n successive transfers, each shifting the edge of the emission line by the amount γ [see the denominator of (8)], corresponding to the width assigned to the energy-transfer rate (2).

Of course, (8) is only valid for $|E| \ll \Delta$, as

otherwise "end effects" arising from the rectangular density of states become important. Equivalently, (8) is only valid for short times. The time scale is set by the requirement that $n\gamma \ll \Delta$, or $W_0 t \gamma \ll \Delta^2$. Using (3), this requires $t \ll \Delta^2 / \pi J^2 W_{\bar{E}-2\bar{A}}$. The right-hand side (see I) is simply the time for a single jump from the center to the edge of the rectangular line.

With this restriction in mind, it is interesting to ask for the time required to make n jumps, such that the width of the emission profile $\Gamma \gg \gamma$ (but still smaller than Δ). Neglecting γ_0 (n large), this requires

$$\begin{aligned} \Gamma &= n\gamma = W_0 \gamma t / \Delta \\ &= \pi J^2 W_{\bar{E}-2\bar{A}} t / \Delta = (\pi J^2 W_{\bar{E}-2\bar{A}} t / \Gamma \Delta) \Gamma. \end{aligned} \quad (9)$$

The term in parentheses is the single-jump probability for an energy change of $(\Gamma \Delta)^{1/2}$. For $\Gamma \gg \gamma$, and Γ a sensible fraction of Δ (say, 0.1Δ), the time required for diffusion to an energy width Γ by n successive "steps" of width γ is close (within a factor of 3) to the time required for a *single* jump to take place over the same energy width Γ . This remarkable feature of our result is a direct consequence of the Lorentzian energy dependence of the energy-transfer rate and the assumption of a constant equilibrium density of states.

Were the energy transfer to fall off sharply with energy mismatch, one would obtain the usual diffusion result (i.e., slow diffusion in small energy-shifting steps). To see this, return to (7) and identify n with the number of steps in the diffusion process. Call the time-evolved emission profile after n steps $P_n(E)$. Then, from (7),

$$P_n(E) \propto \int_{-\infty}^{\infty} [W(s)]^n e^{iEs} ds. \quad (10)$$

If $W(E) = W_0 f(E)$, where $f(E)$ is a sharply varying function of energy, say rectangular with width γ and height $1/\gamma$, the Fourier transform of $W(E)$ could be approximated by

$$\begin{aligned} W(s) &= \frac{1}{\sqrt{2\pi}} \int e^{iEs} W(E) dE \\ &= \frac{W_0}{\sqrt{2\pi}} \frac{1}{\gamma} \int_{-\gamma/2}^{\gamma/2} (1 + iEs - \frac{1}{2}E^2 s^2) dE \\ &= \frac{W_0}{\sqrt{2\pi}} (1 - \frac{1}{24}\gamma^2 s^2) \\ &\approx \frac{W_0}{\sqrt{2\pi}} e^{-\gamma^2 s^2 / 24}. \end{aligned} \quad (11)$$

Equation (11) allows (10) to be written as

$$P_n(E) \propto e^{-6E^2 / \pi^2} = e^{-E^2 / (\pi^2/6)}. \quad (12)$$

This leads to a broadening of the initial excitation after n jumps to a width $\sim n^{1/2}\gamma$. But each step has associated with it the same transition time, so that the width of the distribution proceeds in time as $t^{1/2}$. This is the conventional diffusion result, and is a direct and immediate consequence of the rapid energy dependence of $W(E)$. It is only for a Lorentzian dependence, appropriate to most of the two-phonon-assisted energy-transfer processes developed in I, that the distribution width proceeds linearly in time [and indeed is the same regardless of whether one makes n successive jumps, or a single jump—see (9)].

The situation is different for a Gaussian density of states, as would be the case for ruby. The time development of the line profile is controlled by the density-of-states function—i.e., the Gaussian line shape is controlling over the Lorentzian energy-transfer rate. The evolution of the line profile will be shown in Sec. IV to be a rather simple diminution of the initial excitation profile, with a concomitant increase in intensity of the equilibrium emission line profile.

IV. NUMERICAL SOLUTIONS FOR THE TIME DEVELOPMENT OF THE EMISSION LINE PROFILE FOR ARBITRARY DENSITY OF STATES

The time-development equation for $P(E, t)$, Eq. (1), cannot be solved analytically for arbitrary line shape $g(E)$. If, for example, we should assume that $g(E)$ varies slowly compared to $P(E, t)$ (an assumption only valid for early and intermediate times), we would obtain a diffusionlike differential equation for the Fourier transform of (1):

$$\frac{dP(s, t)}{dt} = -\frac{W_0 \gamma}{\sqrt{2\pi}} \frac{|s|}{\Delta} P(s, t) - \frac{W_0 \gamma}{\sqrt{2\pi}} \frac{|s|}{\Delta^3} \frac{d^2 P(s, t)}{ds^2}. \quad (13)$$

Here, Δ is the width characteristic of $g(E)$, and we have taken $\gamma \ll \Delta$. Unfortunately, we know of no closed-form solution to (13). The presence of s as a coefficient on the right-hand side makes the equation intractable.

As a consequence of our inability to solve (1) analytically, we have had to resort to numerical solutions. We have used an iteration procedure, reducing (1) to

$$P(E, t_n) = P(E, t_{n-1}) + (t_n - t_{n-1}) \int dE' [g(E)W(E - E')P(E', t_{n-1}) - g(E')W(E' - E)P(E, t_{n-1})]. \quad (14)$$

This procedure is valid for very small time intervals $t_n - t_{n-1}$. In order to handle the computer processing expeditiously, we have converted the integral to a sum over 41 values of E' , and sampled the computer memory for the iteration n of interest. For simplicity, we have utilized equal time intervals. Though the time axis is somewhat arbitrary, we have taken the following values for the rate-determining parameters:

$$W_0(t_n - t_{n-1}) = 10^{-3}, \quad \gamma = \gamma_0 = 0.1.$$

The equilibrium line shape has the form

$$g(E) = 0.57 e^{-[1-2.0+(r-1)0.1]^2},$$

where r varies from 1 to 41, defining the energy interval, Gaussian width, and setting the scale for the time interval once $W_0(t_n - t_{n-1})$ is chosen. Note that a change of r by 1 changes E by 0.1.

In order to compare with a physical system, we have related our parameters to the case of 1% ruby. From Sec. II we have $W_0\gamma = \pi J^2 W_{\bar{E}-2\bar{A}}$. But we have taken

$$W_0(t_n - t_{n-1}) \equiv W_0\delta t = 10^{-3} = (\pi J^2 W_{\bar{E}-2\bar{A}}/\gamma^2)\delta t\gamma, \quad (15)$$

where $\gamma = 0.1$. From (2), (15) can be interpreted as δt equaling $\frac{1}{100}$ of the time required to jump an energy difference γ . For 1% ruby, Birgeneau⁵ finds $J \sim 2.5 \times 10^{-3} \text{ cm}^{-1}$, while Blume *et al.*⁶ obtain $W_{\bar{E}-2\bar{A}} = (3 \times 10^9) e^{-42/T} \text{ sec}^{-1}$. An equilibrium emission-line-profile width of 1 cm^{-1} means that $\gamma = 0.1$ corresponds to an energy-transfer width of 0.074 cm^{-1} . Hence,

$$(\pi J^2 W_{\bar{E}-2\bar{A}}/\gamma^2)\delta t = (1.08 \times 10^7) e^{-42/T} \delta t = 10^{-2}.$$

Solving for δt , we find

$$\delta t = (0.93 \times 10^{-9}) e^{42/T} \text{ sec}. \quad (16)$$

At $T = 4.2 \text{ K}$, this implies $\delta t = 10^{-4} \text{ sec}$, while at $T = 10 \text{ K}$, $\delta t = 10^{-7} \text{ sec}$. The figures to be exhibited below are calibrated in units of δt . For lower Cr concentrations (more dilute ruby) J will diminish rapidly, and the time scale will be appropriately expanded.

We exhibit below four examples of the time development of $P(E, t)$, differentiated from one another by virtue of the position in energy of the initial sharp-line excitation. We have chosen initial excitations at $r = 1, 6, 11$, and the line center 21, on Figs. 1-4, respectively. The number displayed for the time t represents the number of increments of δt , hence the number of iterations.

The general features of the time-developed profiles are very interesting. Contrary to the results of Sec. III, the initial sharp-line excitation does not just broaden with increasing time. Rather, on a crude level, the initial pulse simply diminishes

with time, the excitation being transferred to the equilibrium emission line (background) in a more or less uniform manner. [The form of (1) ensures that the integral of $P(E, t)$ is a constant with time. The iterative solution (14) preserves that normalization.]

Closer inspection of the figures reveals interesting variations. The initial excitation line appears to develop a shoulder on the side closer to the equilibrium line center for short times. The shoulder then gradually envelops the entire equilibrium emission profile, after which a "valley" develops between the initial excitation line and the remainder of the line, finally progressing downward so as to separate the two features. All the while the area under the initial excitation is

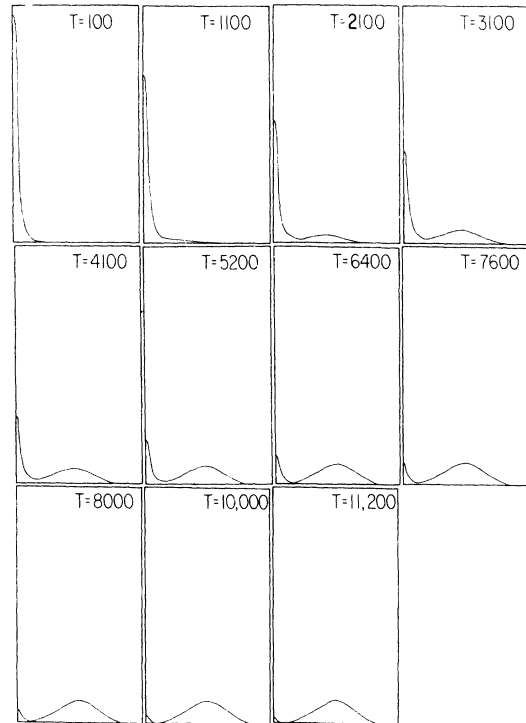


FIG. 1. Representative time evolutions for the emission profile of an inhomogeneously broadened line initially excited at the extreme wing of the line. The transfer rate depends inversely on the square of the energy mismatch, and the explicit numerical factors are defined in the text. The initial excitation was centered at $r = 1$, and the full horizontal scale on the figures is 41. The equilibrium emission line is centered at the center of the figure. The symbol T on each graph denotes the number of time intervals $\delta t = t_n - t_{n-1}$ through which the iteration has progressed. According to (16), $\delta t = 0.93 \times 10^{-9} e^{42/T} \text{ sec}$ for 1% ruby. Thus, at time of 100 (meaning $100\delta t$) translates to 10^{-2} sec at 4.2 K, or 10^{-5} sec at 10 K. For lower concentrations, J diminishes rapidly, and the time scale is appropriately expanded.

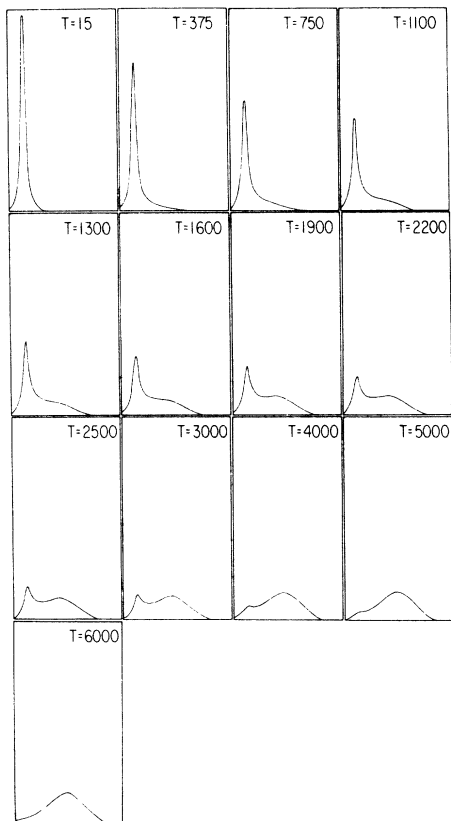


FIG. 2. Same as Fig. 1, but with $r=6$. Note the difference in the time necessary for diffusion to develop the initial sharp-line excitation into the equilibrium emission line profile, as compared to Fig. 1.

diminishing, the area under the equilibrium line shape is increasing. Finally, the initial excitation vanishes, and the equilibrium line shape is fully developed. Yet closer inspection of the figures reveals that the peak of the central line originally is to the left of the equilibrium position, moving gradually to the right as time evolves. Other interesting features are the actual time taken for the diffusion and the intermediate "shapes" of the central portion of the emission profile. A comparison of the figures indicates much more rapid diffusion when the initial excitation is closer to the center of the equilibrium profile. This is the case, clearly, because of the dominating effect of the Gaussian density of states $g(E)$. The larger the density of states in the vicinity of the initial pulse, the more rapid the diffusion process. In fact, the predicted change of the time scale with initial excitation line position may be one of the more crucial tests of our theory. The peculiar shape (see, for example, the case of initial excitation at $r=11$, Fig. 3, where the profile for intermediate times is a skewed triangle) predicted for

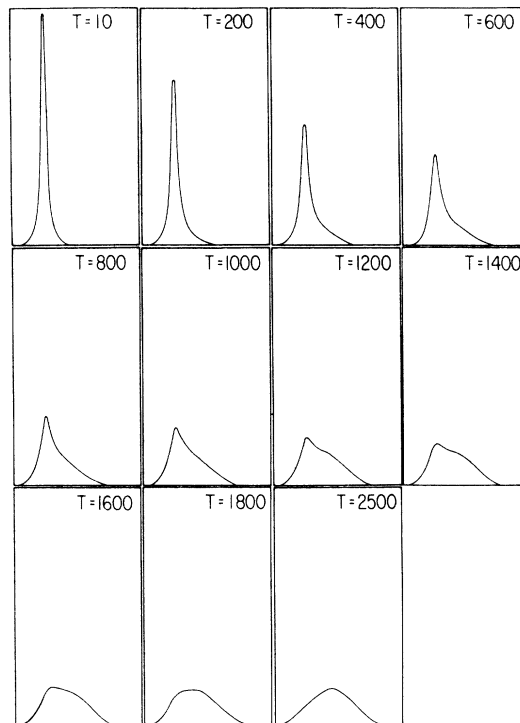


FIG. 3. Same as Fig. 1, but with $r=11$. Again, note the time necessary for complete transfer.

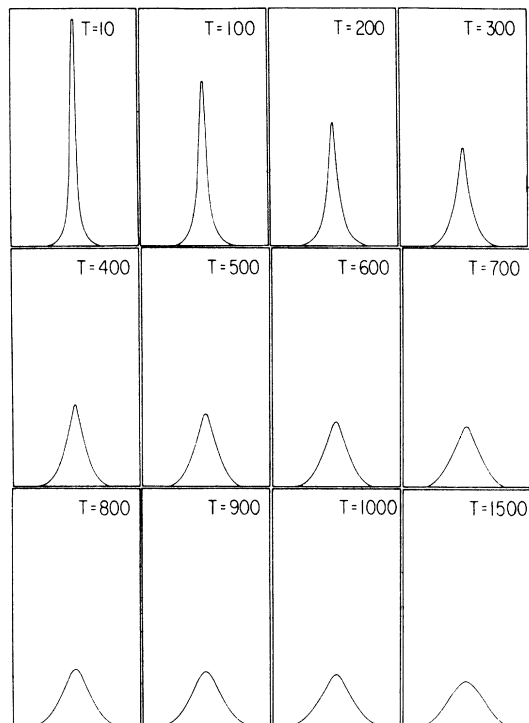


FIG. 4. Same as Fig. 1, but with $r=21$, the position of the equilibrium emission line center. Transfer takes the shortest time for this value of the initial excitation energy.

the line profile at intermediate times can be easily checked experimentally.

Figures 1–4 clearly display the dominating influence of the Gaussian density of states on the time evolution of the line profile. Our exact result in Sec. III, appropriate to a constant density of states, is misleading indeed if one has Gaussian behavior for $g(E)$. The sensitivity of the evolution of the line profile to the exact character of $g(E)$ points to the importance of experiments on systems where the equilibrium inhomogeneous emission profile may depart from Gaussian.

V. SUMMARY

We have examined the temporal character of two-phonon-assisted energy transfer in inhomogeneously broadened lines. We have used the Lorentzian dependence of the energy-transfer rate on energy mismatch, calculated in I, to obtain explicit solutions to the Motegi and Shionoya equation.² We have found that the character of the density of states strongly affects the time development of the emission line profile. A flat (rect-

angular) density of states leads to a monotonic broadening of the initial sharp-line excitation profile, with the interesting property that the broadening rate is nearly independent of the number of diffusion steps involved. When the equilibrium line shape is Gaussian, the energy dependence of the transfer rate is overwhelmed by the exponential character of the density of states, and the latter becomes controlling. There are interesting features associated with the explicit time evolution of the emission line profile.

ACKNOWLEDGMENTS

The authors wish to acknowledge very helpful conversations with Professor W. M. Yen and Professor P. M. Selzer. The interaction between ourselves and their experimental program provided the impetus for our current work. We also wish to thank Professor B. D. Fried for his help in getting us started on the numerical solution of (1), and Steve Gillespie and Ross Bollens for their help in programming.

*Work supported in part by the NSF and by the U.S. ONR, Contract No. N00014-75C-0245. Appreciation is expressed to the Campus Computing Network, University of California, Los Angeles, for allocation of significant computing resources.

¹T. Holstein, S. K. Lyo, and R. Orbach, *Phys. Rev. Lett.* **36**, 891 (1976).

²N. Motegi and S. Shionoya, *J. Lumin.* **8**, 1 (1973).

³T. Holstein, *Phys. Rev.* **72**, 1212 (1947).

⁴See H. Zwibel and T. Holstein, *Bull. Am. Phys. Soc.* **9**, 183 (1964), and H. Zwibel, thesis (University of Pittsburgh, 1965) (unpublished), for a solution of the time decay problem. The stationary case was treated earlier by W. Unno, *Publ. Astron. Soc. Jpn.* **7**, 81 (1955).

⁵R. J. Birgeneau, *J. Chem. Phys.* **50**, 4282 (1969).

⁶M. Blume, R. Orbach, A. Kiel, and S. Geschwind, *Phys. Rev.* **139**, A314 (1965).